

Mechanistic Studies on the Dual Reaction Pathways of Singlet Excited Dibenzoyl(methanato)boron Difluoride (DBMBF₂): Reactions of the Excimer and Exciplexes

Yuan L. Chow,* Shi-Sen Wang, Carl I. Johansson, and Zhong-Li Liu†

Contribution from the Department of Chemistry, Simon Fraser University, Burnaby, British Columbia, Canada V5A 1S6

Received March 29, 1996[⊗]

Abstract: The mechanism of the interaction of singlet excited dibenzoyl(methanato)boron difluoride (*DBMBF₂ = *A) with olefins and substituted benzenes (SB) was investigated by the determination of effective quenching distances (R_{eff}) from fluorescence monitors in acetonitrile as analyzed by the Smoluchowski–Collins–Kimball equation and by solvent effects on the dichotomy of the formation of cycloadducts and [4 + 2] dimers from 1,3-cyclohexadiene (CHD) and 1,3-cyclooctadiene (1,3-COD). The correlation of R_{eff} with $\Delta G_{\text{et}}^{\circ}$ directly demonstrates that the reactants have to get closer to affect electron transfer from these substrates as the driving force become more positive and coalesce on exciplexes. Both photophysical and photochemical probes converge on the partition of encounter pairs to the SSRIP (the k_{et} pathway which leads to radical ion reactions and nonfluorescent) and exciplexes (the k_{ex} pathway which leads to cycloadducts and fluorescent species); the former pathway was promoted by low redox energies of donor–acceptor pairs and by high solvent polarity. The reaction with 1,3-cyclohexadiene gave high quantum yields of the [4 + 2] dimers in acetonitrile and of the cycloadduct in nonpolar solvents; the latter quantum yields were correlated with the solvent polarity parameter $E_{\text{T}}(30)$ in a smooth distribution regardless of pure non-SB or SB solvents or mixture solvents (including benzene), in spite of the fact that the reactive intermediates in the presence of SB are *DBMBF₂–SB exciplexes. It is proposed that in the exciplex the locally excited state provides the driving force in the cycloaddition and the CT state regulates its regioselectivity. The quantum yield of the dimers from CHD was greatly enhanced, reaching their maximum at 12 mol % of *p*-xylene in acetonitrile; the enhancement was attenuated with the addition of toluene and benzene in that order. This shows that the *p*-xylene exciplex underwent extraordinary facile substitution with CHD by electron transfer in acetonitrile probably promoted by superexchange interactions. The *DBMBF₂ excimer reacted with CHD and 1,3-COD to give higher yields of cycloadducts but not the dimers, which must mean that the excimer substitution with CHD proceeds to give the new exciplex but not the radical ion pair. The latter failure as well as that of the benzene exciplex was suggested to arise from the insignificant CT content of the excimer and exciplex. The frontier MO scheme was utilized to rationalize the enhanced reactivity of the exciplexes and excimer on the bases of increased electronic and orbital interactions, respectively.

Introduction

The boron difluorides derived from 1,2-diketones exhibit extensive photoreactivities^{1,2} and photophysical^{3,4} phenomena with various π -bond substrates and have been investigated using dibenzoyl(methanato)boron difluoride (DBMBF₂) as a model compound. Its singlet excited state, *DBMBF₂ is quenched efficiently by aromatic compounds with a concomitant appearance of exciplex fluorescence but forms little product.^{1b} With olefins it undergoes cycloaddition as well as radical ion

formation depending on olefin oxidation potentials;^{1,3} the latter is prone to occur with electron-rich olefins such as 1,3-cyclohexadiene (CHD) in the polar solvent acetonitrile. *DBMBF₂ fluorescence is quenched by CHD (or olefins) without new emission. The dual reaction pathways³ are depicted in Scheme 1 to show photocycloaddition to give adduct **1** and [2 + 4] cycloadduct **2** derived from CHD⁺. The reaction pattern exhibited several unusual features that warrant mechanistic studies. Firstly, as the energy demand for cycloadditions must be much higher than that of electron transfer, it is necessary to find the key intermediate to partition *DBMBF₂ reactivities rationally for the two energetically different pathways. Secondly, the photocycloaddition is an orbital symmetry controlled process in the singlet excited manifold; it is preparatively useful by delivering high quantum yields (particularly when compared with the allied de Mayo reaction) over a wide range of olefins and stereospecific addition products.^{1a} Thirdly, DBMBF₂ gives not only the well-defined singlet excited state but also the anion radical which can be monitored under certain conditions.^{4a} Finally, the interaction of *DBMBF₂ generates distinct exciplex fluorescence with substituted benzenes (SB) (but not with olefins) that enable the study of the role of exciplexes in the overall mechanism.⁴ This paper reports the partition scheme of *DBMBF₂ in the interaction with substrates and the roles played by the excimer and exciplexes in solvents with varying polarity.

† Visiting Professor from National Laboratory of Applied Organic Chemistry, Lanzhou University.

[⊗] Abstract published in *Advance ACS Abstracts*, November 1, 1996.

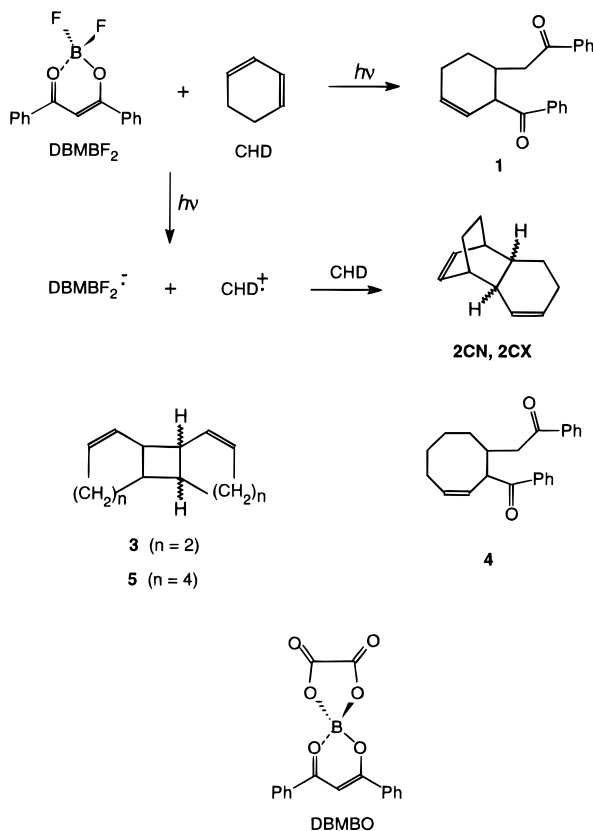
(1) (a) Chow, Y. L.; Cheng, X. *Can. J. Chem.* **1991**, *69*, 1331, 1575. (b) Chow, Y. L.; Ouyang, X. *Can. J. Chem.* **1991**, *69*, 423. (c) Chow, Y. L.; Wang, S. S. *Can. J. Chem.* **1993**, *71*, 846.

(2) (a) Chow, Y. L.; Cheng, X.; Johansson, C. I. *J. Photochem. Photobiol. A: Chem.* **1991**, *57*, 247. (b) Ilge, H. D.; Birkener, E.; Fassler, D.; Kozmenko, M. V.; Kanzmin, M. G.; Hortman, H. *J. Photochem.* **1986**, *32*, 177; (c) Schade, W.; Ilge, H. D.; Hartman, H. *J. Prakt. Chem.* **1986**, *328*, 941.

(3) (a) Chow, Y. L.; Wang, S. S.; Liu, Z. L.; Wintgens, V.; Valat, P.; Kossanyi, J. *New J. Chem.* **1994**, *18*, 923. (b) Chow, Y. L.; Wang, S. S. *Tetrahedron Lett.*, **1994**, *35*, 9661 (a brief account of solvent effects is communicated here).

(4) (a) Liu, Z. L.; Zhang, M. X.; Yang, L.; Liu, Y. C.; Chow, Y. L.; Johansson, C. I. *J. Chem. Soc., Perkin Trans. 2* **1994**, 585. (b) Chow, Y. L.; Johansson, C. I. *J. Phys. Chem.* **1995**, *99*, 17558, 17566. (c) Harju, T. O.; Erostyak, J.; Chow, Y. L.; Koppi-Tommola, J. E. I. *Chem. Phys.* **1994**, *181*, 259.

Scheme 1



Results

The Weller-Type Correlation. In acetonitrile, $^*\text{DBMBF}_2$ fluorescence intensities (I_0 and I) were proportionally quenched by a substrate in a low concentration range according to eq 1,

$$I_0/I = 1 + K_{\text{SV}}[D] = 1 + k_{\text{obs}}\tau_m[D] \quad (1)$$

the Stern–Volmer equation,⁵ in which the quenching efficiency is represented by K_{SV} ; the observed rate constant, k_{obs} , is the composite of rate constants related to exciplex formation and decays, and τ_m is the lifetime of $^*\text{DBMBF}_2$ (see Scheme 2 later). While quenching by olefins leads to straightforward reduction of intensities, that by SB induces new exciplex fluorescence at the longer wavelength; examples were published before.^{3a,4b} For SB of poorer electron donors than toluene, fluorescence intensities, owing to poor resolution of emission spectra, were determined by another procedure.⁶ In the low concentration range of substrates (<0.2 M), these Stern–Volmer plots gave good straight lines to afford K_{SV} with the unity intercept and were used to calculate k_{obs} from $\tau_m = 0.30$ ns, the intrinsic lifetime in the $[\text{DBMBF}_2] < 10^{-3}$ M region. In analogy to Weller's model of electron transfer,⁵ $\log k_{\text{obs}}$ was correlated with $\Delta G_{\text{et}}^{\circ} = E_{\text{ox}} - E_{\text{red}} - E_s - C$ where $C = 0.06$, $E_{\text{red}} = -0.91$,

and $E_s = 3.19$ eV for DBMBF_2 . These values from SB and olefins are listed in Table 1 and are plotted in Figure 1A to show their smooth variation together.

Rehm and Weller^{5c,d} have proposed that excited state quenching rate constants by electron transfer from encounter pairs can be computed from reorganizational free energy $\Delta G_{\text{et}}^*(0)$ ($= 0.12$ eV) and k_{diff} ($= 2.5 \times 10^{10} \text{ M}^{-1} \text{ s}^{-1}$); the calculated rate constants were drawn as the solid line in Figure 1. The continuous plot of $\log k_{\text{obs}}$ from SB as well as olefins clearly demonstrated two regions; the exergonic region at $\Delta G_{\text{et}}^{\circ} < -0.35$ eV that exhibits rate constants in the domain of the diffusion-controlled limit in agreement with the RW prediction. The substrates of this region interacted with $^*\text{DBMBF}_2$ to show primarily cation radical reactions (for olefins)^{1a} and simple fluorescence quenching without exciplex emission^{4b} for SB in acetonitrile; these are shown as solid dots in Figure 1. The endergonic region of $\Delta G_{\text{et}}^{\circ} > -0.35$ eV showed that k_{obs} began to fall from the diffusion limit but was much higher than the RW prediction. In the endergonic region, $^*\text{DBMBF}_2$ interacted with those olefins to give the cycloadducts^{1a} and with SB fluorescent exciplexes^{4b} in acetonitrile; those points are shown as open circles in Figure 1. The transition to endergonic mode was smooth involving all experimental points. For comparison, dibenzoyl(methano)boron oxalate (DBMBO, $E_{\text{red}} = -0.64$ eV),⁷ a better electron acceptor, was also studied in a manner similar to give some experimental points that were obviously placed closer to the calculated RW line. As k_{obs} in the exergonic region could not demonstrate the efficiency of fluorescence quenching in response to the decreasing $\Delta G_{\text{et}}^{\circ}$ owing to the diffusion-controlled limitation, we resorted to interrogating the distance of $^*\text{DBMBF}_2$ to substrates at which fluorescence quenching occurs in this domain, where the diffusion parameters must be reasonably constant provided structurally similar substrates are involved.

Effective Quenching Distance. In the higher concentration range of $[\text{substrate}] > 0.2$ M, Stern–Volmer quenching plots of $^*\text{DBMBF}_2$ by olefins or SB showed distinct upward curvatures that are more pronounced with increasing electron donating abilities of substrates (Figure 2). The curvature could arise from transient effects⁸ and/or ground state electron donor–acceptor (EDA) complex formation.^{8a,c} Though DBMBF_2 does form EDA complexes with mesitylene or better donors, their K_a ($<0.14 \text{ M}^{-1}$)⁹ is too small to cause significant deviation from linearity in Stern–Volmer plots. Assuming $K_{\text{SV}} = 10 \text{ M}^{-1}$ and EDA molar absorptivity as big as that of DBMBF_2 , at the concentrations used in these quenching experiments at $[\text{DBMBF}_2] = 10^{-5}$ M and $[\text{SB}] = 0.1$ M, the deviation can be estimated to be less than 1%. Since most EDA molar absorptivities are far smaller than the substrates themselves, we could conclude that the EDA formation did not cause the curvatures in Figure 2.

The transient effects of diffusion-controlled reactions have their origin in the time evolution of concentration gradients in quenching environments^{9a} and occur in diffusion-controlled quenching of excited species with lifetime shorter than 2 ns as

(5) (a) Leonhardt, H.; Weller, A. *Ber. Bunsen-Ges. Phys. Chem.* **1963**, 67, 791. (b) Knibbe, H.; Rehm, D.; Weller, A. *Ber. Bunsen-Ges. Phys. Chem.* **1968**, 72, 257. (c) Rehm, D.; Weller, A. *Ber. Bunsen-Ges. Phys. Chem.* **1969**, 73, 834. (d) Rehm, D.; Weller, A. *Isr. J. Chem.* **1970**, 8, 259. (e) Weller, A. In *Fast Reactions and Primary Processes in Chemical Reactions: Nobel Symp. 5*; Claesson, S., Ed.; Interscience: New York, 1967; p 413. (f) Weller, A. *Z. Phys. Chem. N. F.* **1982**, 133, 93. (g) Weller, A. *Z. Phys. Chem. (Munich)* **1982**, 130, 129; (h) Knibbe, H.; Röllig, K.; Schäfer, F. P.; Weller, A. *J. Chem. Phys.* **1967**, 47, 1184. (i) Rehm, D.; Weller, A. *Z. Phys. Chem. N. F.* **1970**, 69, 183. (j) Knibbe, H.; Rehm, D.; Weller, A. *Ber. Bunsen-Ges. Phys. Chem.* **1969**, 73, 839. (k) Weller, A. *The Exciplex*; Gordon, M., Ware, W. R., Eds.; Academic: New York, 1975.

(6) Walker, M. S.; Bednar, T. W.; Lumbry, R. *J. Chem. Phys.* **1967**, 47, 1020.

(7) Chow, Y. L.; Zhang, Y. H.; Gautron, R.; Yang, L.; Rassat, A.; Yang, S. Z. *J. Phys. Org. Chem.* **1996**, 9, 7.

(8) (a) Rice, S. A. In *Comprehensive Chemical Kinetics: Diffusion-Limited Reactions*; Bamford, C. H., Tpper, C. F. H., Compton, R. G., Eds.; Elsevier: Amsterdam, 1985; Vol. 25. (b) Szabo, A. *J. Phys. Chem.* **1989**, 93, 6929. (c) Viriot, M. L.; Andre, J. C.; Ware, W. R. *J. Photochem.* **1980**, 14, 133. Andre, J. C.; Niclaude, M.; Ware, W. R. *Chem. Phys.* **1978**, 28, 371. (d) Stevens, B.; McKeithan, D. N. *J. Photochem. Photobiol. A: Chem.* **1987**, 40, 1; **1989**, 47, 131. (e) Eads, D. D.; Dismer, B. G.; Fleming, G. R. *J. Chem. Phys.* **1990**, 93, 1136. (f) Song, L.; Dorfman, R. C.; Swallen, S. F.; Fayer, M. D. *J. Phys. Chem.* **1991**, 95, 3454. (g) Dutt, G. B.; Periasamy, N. *J. Chem. Soc., Faraday Trans.* **1991**, 87, 3815.

(9) Johansson, C. J. Ph.D. Dissertation, Simon Fraser University, 1994.

Table 1. Quenching of DBMBF₂ (2×10^{-6} M) Fluorescence in Acetonitrile

	benzene	E_{ox} (V vs SCE) ^a	ΔG_{ET}° (eV) ^b	K_{SV} (M ⁻¹)	k_{obs} (10^9 M ⁻¹ s ⁻¹) ^c	D_{DA} (cm ² s) ^d	R_{VWD} (Å) ^e	R_{eff} (Å)
1	hexamethylbenzene	1.59	-0.75	9.94	33.1	4.39	7.29	6.1 ± 0.9
2	pentamethylbenzene	1.71	-0.63	9.00	30.0	4.53	7.18	5.6 ± 0.8
3	durene	1.79	-0.55	7.36	24.5	4.69	7.06	5.2 ± 0.8
4	1,2,3,5-tetramethylbenzene	1.83	-0.51	7.47	24.9	4.69	7.06	5.2 ± 0.8
5	1,2,3,4-tetramethylbenzene	1.82	-0.52	7.56	25.2	4.69	7.06	4.8 ± 0.7
6	1,2,4-trimethylbenzene	1.92	-0.42	7.02	23.4	4.85	6.92	4.2 ± 0.6
7	mesitylene	2.02	-0.32	5.81	19.4	4.85	6.92	3.8 ± 0.6
8	<i>p</i> -xylene	2.06	-0.28	5.03	16.8	5.09	6.78	3.5 ± 0.5
9	<i>m</i> -xylene	2.14	-0.20	4.03	13.4	5.09	6.78	3.3 ± 0.5
10	<i>o</i> -xylene	2.13	-0.21	4.29	14.3	5.09	6.78	3.2 ± 0.5
11	toluene	2.25	-0.09	2.65	8.83	5.23	5.23	
12	chlorobenzene	2.48	0.14	0.91	3.0			
13	benzene	2.62	0.28	0.54	1.8			
14	methylbenzoate	2.69	0.35	0.53	1.8			
15	cyanobenzene	2.94	0.60	0.16	0.5			
16	quadricyclane	0.91	-1.43	10.6	35.3	5.96	6.48	5.4
17	2,5-dimethyl-2,4-hexadiene	0.98	-1.36	10.1	33.7	4.84	6.93	6.0
18	α -pinene	1.41	-0.93	7.46	28.2	4.72	7.07	4.8
19	2,5-norbornadiene	1.56	-0.80	6.51	21.7	5.73	6.57	3.8
20	1,3-cyclohexadiene	1.53	-0.81	8.66	28.9	5.72	6.59	4.8
21	2,4-dimethyl-1,3-pentadiene	1.62	-0.72	7.62	25.4	5.20	6.79	4.6
22	2-methylcyclohexene	1.70	-0.64	5.43	18.1	5.27	6.75	3.6
23	1,3-pentadiene	1.73	-0.61	6.01	20.0	5.73	6.45	3.5
24	1,3-cyclooctadiene	1.89	-0.45	6.20	20.7	5.07	6.83	4.1
25	β -pinene	1.89	-0.45	4.74	15.8	4.72	7.07	3.6
26	norbornene	2.02	-0.32	3.65	12.2	5.48	6.64	(2.60)
27	cyclohexene	2.14	-0.20	3.59	12.0	5.64	6.59	2.94
28	cycloheptene	(2.14)	(-0.20)	3.70	12.3	5.34	6.75	(2.70)
29	anethole	1.11	-1.23	11.6	38.7	4.70	7.04	6.6
30	1,4-dimethoxybenzene	1.49	-0.85	10.0	33.3	4.98	6.88	5.80
31	triethylamine	1.15	-1.19	10.4	34.7	5.14	6.87	5.7

^a The oxidation potentials are measured in our group if not cited; 1-12 from ref 17a, 1-4, 6, and 8 from ref 17b, 16, and 19 from ref 17c, 17 from ref 17d, 18, 22, and 25-27 from ref 17e, 20, and 23-29 from ref 17f, and 31 from ref 17g; 21 and 30 calculated from $E_{ox} = 1.369IP - 10.29$ eV; 28 is assumed to be the same as 27. ^b Calculated from $\Delta G_{et}^{\circ} = E_{ox} - E_{red} - E_s - C = E_{ox} - (-0.91) - 3.19 - 0.06$ eV. ^c Calculated from K_{sv}/τ_m , where $\tau_m = 0.30$ ns. ^d Calculated from ref 11. ^e Calculated from atomic increments (ref 10).

a necessary condition. The steady-state equation developed from the theory of such effects based on a continuum model is known as Smoluchowski-Collins-Kimball (SCK) equation,^{8a,b} eq 2, where where $\exp(V[D])$ is the Perrin modification term.^{8c}

$$I_0/I = (1 + 4\pi R_{eff} D_{AD} N_A [D] \tau_m) Y^{-1} \exp(V[D]) \quad (2)$$

$$Y = 1 - (b/a^{1/2}) \pi^{1/2} \exp(b^2/a) \operatorname{erfc}(b/a^{1/2}) \quad (2a)$$

$$a = (\tau_m)^{-1} + 4\pi R_{eff} D_{AD} [D] N_A \quad (2b)$$

$$b = 4\pi (R_{eff})^2 D_{AD} [D] (\pi D_{AD})^{-1/2} N_A \quad (2c)$$

$$V = (4\pi/3) ((R_{eff})^3 - (R_{VDW})^3) \quad (2d)$$

The SCK equation predicts Stern-Volmer quenching ratios as the function of the sum of diffusion coefficients, D_{AD} , and the effective fluorescence quenching distance, R_{eff} , in addition to the substrate concentration $[D]$. The necessary parameters R_{VDW} were calculated from the method by Edward,¹⁰ and D_{AD} from the data and method described by Chan and Chan,¹¹ and listed in Table 1. R_{eff} was systematically varied in eq 2 until the best fit was achieved with plots in Figure 2. Sensitivity computations showed that a 10% variation in either D_{AD} or R_{VDW} parameters caused less than 15% fluctuations for R_{eff} ; these figures may be taken as an error margin for R_{eff} in Table 1. R_{eff} of all substrates showed electron transfer in the exergonic region occurring from about 7 Å to the exciplex distance of about 3.0

Å (Figure 1B); shorter R_{eff} than this must come from increasing error as deviation from the diffusion controlled rate constant become greater near the ΔG_{et}° value corresponding to trimethylbenzenes or greater. In contrast to the smooth distribution of R_{eff} points from SB, those from olefin quenching exhibited scatter and shorter distances; these could arise from structural diversity and the higher reorganizational energies required in olefin quenching. At this point it is useful to introduce the mechanistic representation as in Scheme 2, which is an adaptation from that proposed by the Eastman Kodak group;¹² the exciplex is shown as $|A^-D^+ \leftrightarrow *AD\rangle = *(AD)$, encounter complexes as $*A(S)D$, and solvent separated radical ion pairs (SSRIP) as $A^-(S)D^+$. The definition and physical meaning of this scheme follow the original proposal;^{12e} reacting species $*A$ and D approach from the right to the contact distance in exciplexes at the left, and energy levels increase vertically.

Solvent Effects on Quantum Yields. It was noted that the fluorescence intensities of $*DBMBF_2$ exciplexes tended to be higher in complexes with SB of higher oxidation potentials (see Figure 1A, open circles and triangles); these increased very much in nonpolar solvents in which unusually high fluorescence quantum yields of $*DBMBF_2$ exciplexes were noted in cyclohexane.^{4b} Similar trends were noted for similar exciplexes from 2,6,9,10-tetracyanoanthracene and 9,10-dicyanoanthracene¹² and other fluorophores.¹³⁻¹⁶ For anthracene-type exciplexes, the Eastman Kodak Group^{12a,e} defined $k_{ex}/(k_{ex} + k_{et})$ as the

(12) (a) Gould, I. R.; Young, R. H.; Mueller, L. J.; Farid, S. *J. Am. Chem. Soc.* **1994**, *116*, 8176. (b) Gould, I. R.; Young, R. H.; Mueller, L. J.; Albrecht, A. C.; Farid, S. *J. Am. Chem. Soc.* **1994**, *116*, 8188. (c) Gould, I. R.; Farid, S. *J. Phys. Chem.* **1992**, *96*, 7635. (d) Gould, I. R.; Young, R. H.; Moody, R. E.; Farid, S. *J. Phys. Chem.* **1991**, *95*, 2068. (e) Gould, I. R.; Mueller, L. J.; Farid, S. *Z. Phys. Chem.* **1991**, *170*, 143.

(13) Watkins, A. R. *J. Phys. Chem.* **1979**, *83*, 1892.

(10) Edward, J. T. *J. Chem. Educ.* **1970**, *47*, 261.

(11) Chan, T. C.; Chan, M. L. *J. Chem. Soc., Faraday Trans.* **1992**, *88*, 2371.

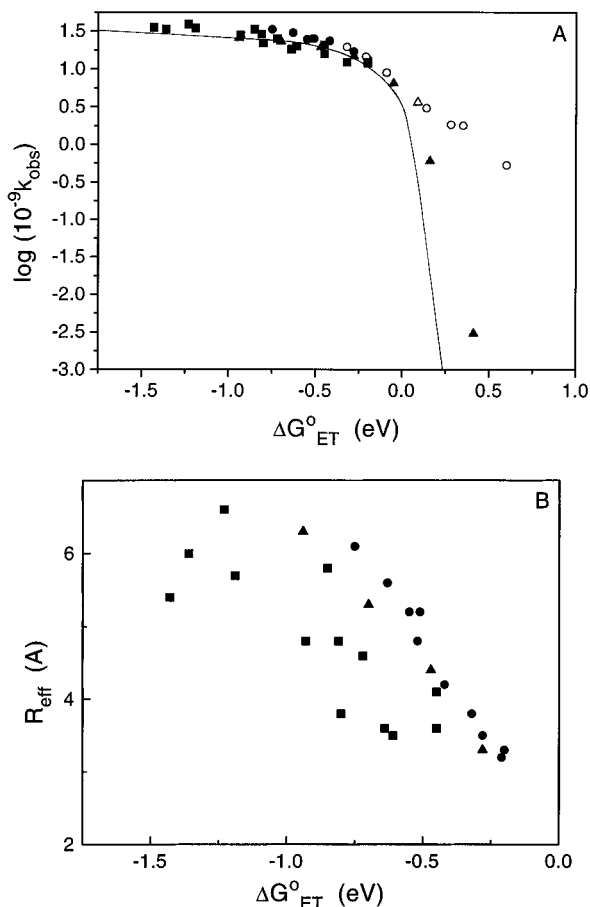


Figure 1. (A) Plot of $\log k_{\text{obs}}$ of DBMBF₂ fluorescence quenching by SB (solid dots: circles for those showing exciplex emission) and by olefins (squares); the corresponding data of *DBMBO–SB in acetonitrile are shown as solid and open triangles; for calculations of ΔG_{ET}^0 and k_{obs} see the text. (B) The plot of R_{eff} vs ΔG_{ET}^0 .

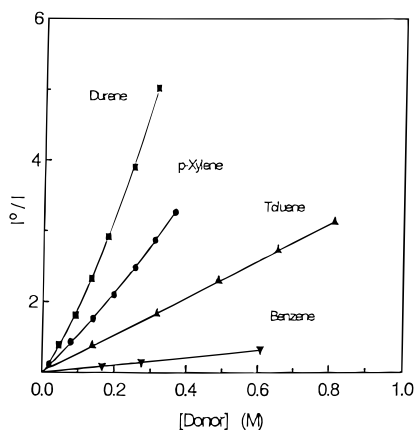


Figure 2. The Stern–Volmer plot of the quenching of DBMBF₂ (2×10^{-6} M and $\lambda_{\text{ex}} = 365$ nm) fluorescence by substituted benzenes in acetonitrile.

efficiency α with which the exciplex is formed from encounter pairs as in Scheme 2; α is unity in less polar solvents to indicate efficient exciplex formations in the bimolecular kinetics.^{12a} The *DBMBF₂ reaction pattern could be studied as a function of solvent polarity, particularly in solvents less polar than acetonitrile.

In nonpolar solvents, such as ether- and benzene-type solvents, *DBMBF₂ reacted with CHD to give cycloadduct **1**

(14) Prochorow, J.; Bernard, E. *J. Lumin.* **1974**, *8*, 471.

(15) Pac, C.; Yasuda, M.; Shima, K.; Sakurai, H. *J. Chem. Soc. Jpn.* **1982**, *55*, 1605.

Scheme 2

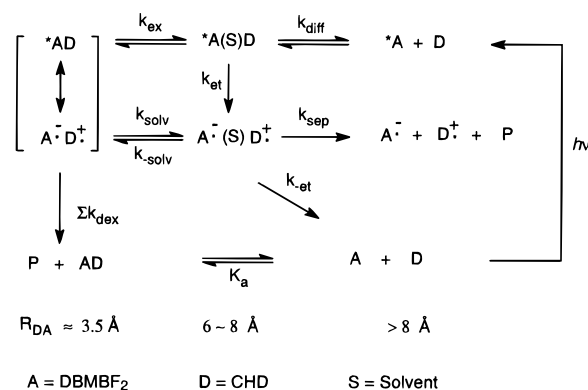


Table 2. Quantum Yield of the DBMBF₂–CHD Photoreaction in Pure Solvent

solvent ^a	$E_{\text{T}}(30)$	$10^3\Phi_{\text{a}}$ of 1	$10^3\Phi_{\text{d}}$ of 2	2CN/2CX
CH ₃ CN	45.6	0.28	70.0	7.4
acetone	42.2	0.60	7.9	4.9
CH ₂ Cl ₂	40.7	1.66	55.6	3.9
THF	37.4	1.88	1.8	0.3
THP	36.6	4.52	1.2	0.4
dioxane	36.0	3.02	1.4	0.6
ether	34.5	11.5	1.5	1.0
benzene	34.3	14.7	13.5	2.7
toluene	33.9	22.3	9.0	2.5
<i>p</i> -xylene	33.1	25.9	10.7	2.1

^a Samples of [DBMBF₂] = 0.03 M and [CHD] = 0.30 M in aromatic solvents were irradiated under N₂ at 350 nm for 30 min and in nonaromatic solvents for 2 h.

and [4 + 2] dimers **2CN** and **2CX** (*cis-endo* and *cis-exo*). In more polar solvents, adduct **1** decreased and dimer **2** (mostly *cis-endo*) increased drastically; in acetonitrile, **1** was barely detectable by GC analysis and only **2** was isolated (Table 2). In this photoreaction, [2 + 2] dimers **3** were also obtained in small quantum yields (0.004–0.007) that varied little under wide conditions; dimers **3** (as well as **2CX**) have been shown to arise from triplet state CHD independent of solvent changes by sensitization experiments.^{3a} The photoreaction of DBMBF₂ with 1,3-cyclooctadiene (1,3-COD) gave adduct **4** showing similar quantum yield dependency to polarity, but under all conditions used, the yields (< 1%) of [2 + 2] dimers **5** were poor. While under the present photolysis conditions, electron transfer to 1,3-COD (estimated $E_{\text{ox}} 1.89$ eV)^{3a} could occur, expected [4 + 2] dimers initiated by 1,3-COD^{•+} have not been observed or reported.^{17f}

Owing to the fact that dimers **2** were formed by a chain process, Φ_{d} was dependent on a number of factors and could not be reliably used in correlation. Quantum yields (Φ_{a}) of adduct **1** (and **4**) were free from such mechanistic complications and were determined under a set of fixed conditions (including concentrations) in various solvents. In Figure 3 $\ln(1/\Phi_{\text{a}})$ for **1** is plotted against solvent polarity parameters $E_{\text{T}}(30)$, which use the absorption maxima (in kcal/mol) of the CT band of a betaine to represent the overall polarity of solvents.¹⁸ Within experi-

(16) (a) Jones, C. R.; Allman, B. J.; Mooring, A.; Spahic, B. *J. Am. Chem. Soc.* **1983**, *105*, 652. (b) Yang, N. C.; Srinivasan, K. *J. Am. Chem. Soc.* **1975**, *97*, 5006.

(17) (a) Schlessener, C. J.; Amatore, C.; Kochi, J. K. *J. Phys. Chem.* **1986**, *96*, 3747. (b) Gould, I. R.; Ege, D.; Moser, J. E.; Farid, S. *J. Am. Chem. Soc.* **1990**, *112*, 4290. (c) Gassman, P. G.; Yamaguchi, R. *J. Org. Chem.* **1978**, *43*, 4392. (d) Kubo, Y.; Suto, M.; Araki, T. *J. Org. Chem.* **1986**, *51*, 4404. (e) Shono, T.; Ikeda, A. *J. Am. Chem. Soc.* **1972**, *94*, 7892. (f) Bauld, N. L.; Harichian, B.; Reynolds, D. W.; White, J. C. *J. Am. Chem. Soc.* **1988**, *110*, 8111. (g) Murov, S. L.; Carmichael, I.; Hug, G. L. *Handbook of Photochemistry*; Marcel Dekker, Inc.: New York, 1993; p 269.

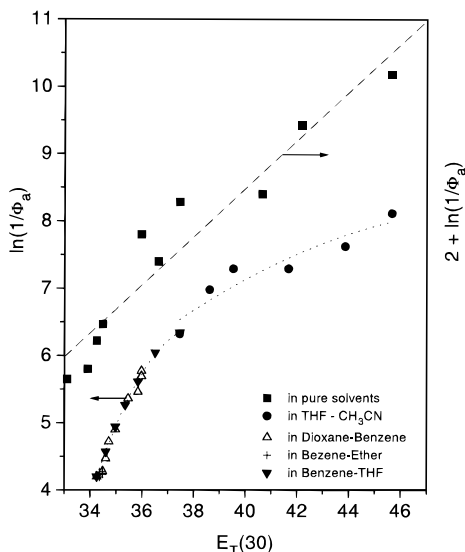


Figure 3. Plot of $\ln(1/\Phi_a)$ for **1** from the CHD photoreaction against the polarity parameters $E_T(30)$ of pure and mixture solvents.

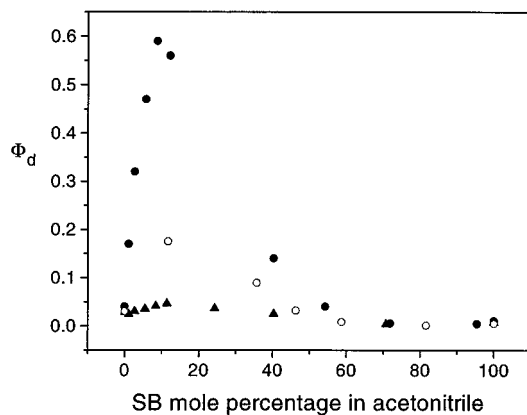


Figure 4. Plot of the quantum yield of dimers **2** (Φ_d) in mixture solvents of *p*-xylene (●), toluene (○) and benzene (▲) in CH_3CN .

mental errors of GC analysis, a smooth increase of Φ_a along the polarity continuum could be traced. In order to distinguish solvent effects of specific and nonspecific types, both quantum yields Φ_a and Φ_d were also determined in solvent mixtures as listed in Table 2A (Supporting Information). Using the estimated $E_T(30)$ (from proportionality to mol %), these Φ_a in nonaromatic solvent mixtures (case I) and those in benzene–ether-type mixtures (case II) could be fit into the plot generated by pure solvents (see Figure 3). Case III consists of the mixtures of highly polar acetonitrile with toluene and *p*-xylene (*i.e.*, better electron donors than benzene), where the quantum yield of dimers **2** were enhanced to reach the maxima in the 12 mol % region; indeed $\Phi_d \approx 1.0$ was recorded with $[\text{CHD}] \approx 0.2 \text{ M}$ at the 5~10% conversion. Such Φ_d enhancements were exceptionally large in the mixtures with *p*-xylene but attenuated in those with toluene and benzene as shown in Figure 4. Though Φ_a of adduct **1** in these acetonitrile mixtures appears to be increased as in Table 2A, the quantity range is too small to be accurately measured.

The photoreaction of DBMBF_2 with 1,3-COD was investigated in a manner similar to that for solvent effects on the quantum yield (Φ_a) of **4** only; Φ_d for dimer **5** was low, not relevant, and was ignored. The distribution of points for the $\ln(1/\Phi_a)$ vs $E_T(30)$ plot (Figure 5) in pure solvents and the acetonitrile–dioxane mixtures was indistinguishable.

Kinetic Studies. Since $^*\text{DBMBF}_2$ formed the transient excimer extensively in nonaromatic solvents at concentrations

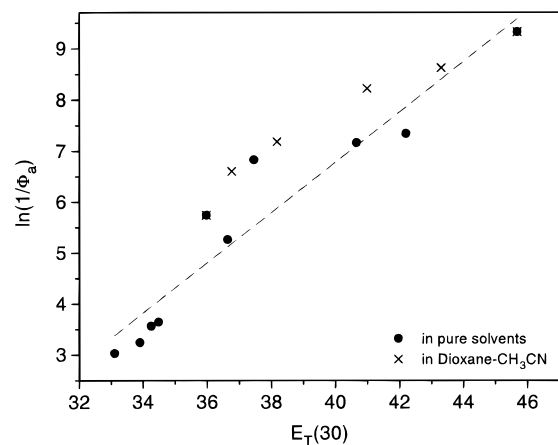


Figure 5. Plot of $\ln(1/\Phi_a)$ for **4** from the 1,3-COD photocycloaddition against $E_T(30)$ of pure and mixture solvents.

used in preparative photoreactions, the Stern–Volmer quenching efficiency by dienes was investigated with $[\text{DBMBF}_2] 10^{-6}$ – 0.1 M in order to examine the reactive intermediate. Taking advantage of good fluorescence intensities, eq 1 was used to calculate K_{SV}^{m} for the quenching of $^*\text{DBMBF}_2$ monomer peaks at 415–430 nm; in this case, $\tau_{\text{m}} = (\sum k_{\text{m}1} + k_{\text{m}}[\text{DBMBF}_2])^{-1}$, $\sum k_{\text{m}1}$ is the sum of all unimolecular reaction rate constants of $^*\text{DBMBF}_2$, and $k_{\text{m}} (= 2.7 \times 10^{10} \text{ M}^{-1} \text{ s}^{-1})$ is the bimolecular rate constant of the excimer formation.^{1a} $K_{\text{SV}}^{\text{em}}$ for excimer quenching was calculated from eq 3 developed by Caldwell's

$$(I_o/I)_{\text{ex}}/(I_o/I)_{\text{m}} = 1 + K_{\text{SV}}^{\text{em}} [\text{D}] \quad (3)$$

group; $(I_o/I)_{\text{ex}}$ and $(I_o/I)_{\text{m}}$ are the intensity quenching ratios monitored at the excimer (*ca.* λ 520 nm) and monomer (λ 430 nm) peaks, respectively, as shown in Figure 6. In benzene, $^*\text{DBMBF}_2$ –benzene exciplex (λ 424 nm) was quenched by dienes in a straightforward pattern to afford $K_{\text{SV}}^{\text{ex}}$ by eq 1, in which τ_{m} now is the exciplex lifetime of 2.1 ns in benzene. The K_{SV} values are summarized in Table 3. These K_{SV} values could be determined also by measuring the quantum yields of Φ_a at various diene concentrations and by performing double-reciprocal plots according to eq 4; $K_{\text{SV}} = \text{intercept/slope}$.

$$1/\Phi_a = 1/\beta + 1/(\beta K_{\text{SV}}[\text{D}]) \quad (4)$$

Unfortunately with increasing $[\text{CHD}]$, (i) Φ_d fluctuated greatly making the analytical errors for Φ_a too large to be used in eq 4 and (ii) Φ_a changed little (in benzene and dioxane) or even decreased (in THF), indicating the possible occurrence of quenching of the exciplex by CHD itself. For 1,3-COD, Φ_a was high enough to be determined; the plot according to eq 4 gave K_{SV} (=intercept/slope) of 10.3 and 3.1 M^{-1} in benzene and dioxane, respectively; these agreed well with those derived from fluorescence monitor in Table 3. The details of these plots are given in the thesis submitted by SSW.¹⁹

The quantum yields of **1** and **4** were determined in dioxane and methylene chloride with increasing $[\text{DBMBF}_2]$ at 0.01~0.07 M under the fixed conditions at $[\text{diene}] = 0.3 \text{ M}$: that at $[\text{DBMBF}_2] = 0.01 \text{ M}$ was arbitrarily taken as the reference $\Phi_{0.01}$. The quantum yield ratio $(\Phi/\Phi_{0.01})_a$ increased with increasing $[\text{DBMBF}_2]$ as shown in Figure 7. These plots indicated that in nonaromatic solvents, an additional reaction channel to give the adducts was generated as $[\text{DMBBF}_2]$ rose,

(18) Reichardt, C. *Solvents and Solvent Effects in Organic Chemistry*; VCH Publishers: New York, 1988; pp 365–371.

(19) Wang, S.-S. Ph.D. Dissertation, Simon Fraser University, August 1996.

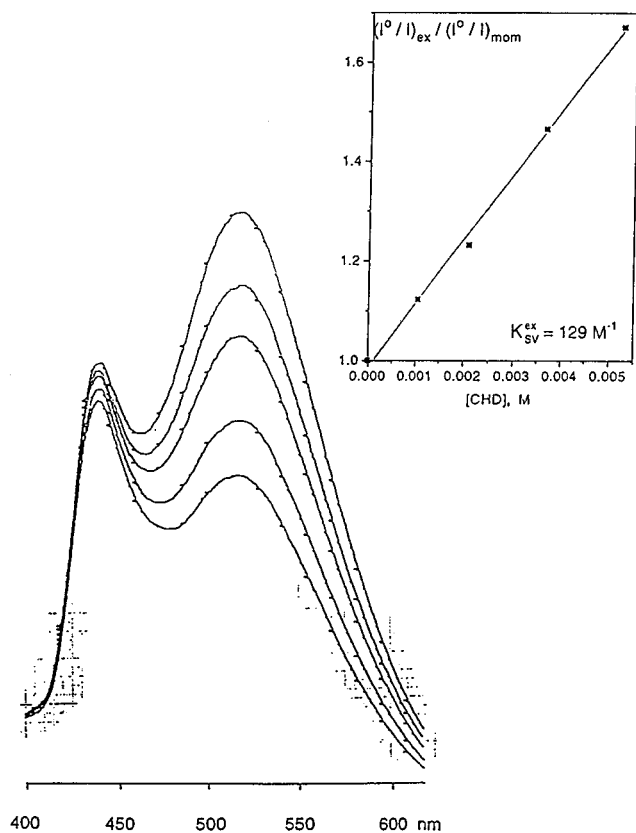


Figure 6. Quenching of DBMBF₂ (0.20 M) fluorescence in THF (λ_{ex} 365 nm) by CHD and the corresponding Stern–Volmer plot.

Table 3. Stern–Volmer Quenching Efficiency of DBMBF₂ Fluorescence by Dienes

solvent	[DBMBF ₂], M (λ_{moni})	K_{SV}	
		by CHD	by 1,3-COD
THF ^a	5×10^{-6} (417 nm)	11.6 ± 0.3	8.1 ± 0.3
THF ^b	0.20 (522 nm)	129 ± 4	52 ± 2
dioxane ^a	0.03 (432 nm)	10.6 ± 0.4	3.8 ± 0.2
dioxane ^a	5×10^{-6} (417 nm)		3.7 ± 0.2^d
benzene ^c	5×10^{-6} (424 nm)	20.6 ± 1.0	10.2 ± 0.5^d
benzene ^c	0.03 (424 nm)	21.4 ± 1.1	8.8 ± 0.4

^a K_{SV}^{m} values. ^b $K_{\text{SV}}^{\text{em}}$ values. ^c $K_{\text{SV}}^{\text{ex}}$ values. ^d $K_{\text{SV}} = 3.1$ and 10.3 M^{-1} in dioxane and benzene, respectively, by quantum yield monitor of adduct **4**.

and was assumed to be the excimer reaction. In contrast, the similar plots of $(\Phi/\Phi_{0.01})_{\text{a}}$ in benzene showed marginal increases, indicating that the ^{*}DBMBF₂–benzene exciplex is the sole transient reacting with dienes to give the adducts. The quantum yield of **2** (Φ_{d}) was also determined under similar conditions with the increasing [DBMBF₂] = 0.01–0.1 M. In dioxane, Φ_{d} varied randomly between 0.005 and 0.004, and in acetonitrile, 0.085 ± 0.003 : they clearly showed that Φ_{d} was independent of DBMBF₂ concentration changes, that is, $(\Phi/\Phi_{0.01})_{\text{d}} \approx 1$. The results clearly demonstrated that the excimer does not react with CHD by electron transfer even in acetonitrile.

Discussion

The kinetic studies by fluorescence quenching measurements indicate that not only ^{*}DBMBF₂ but both the excimer and the exciplexes also interact with dienes. In benzene (or SB solvent), no doubt, the corresponding exciplex is the reactive intermediate as shown by the agreement of K_{SV} values for 1,3-COD from two measurements (see Table 3); the reaction with CHD could not be proven by this method owing to unknown secondary reactions (but see below). The $K_{\text{SV}}^{\text{em}}$ values for the excimer are

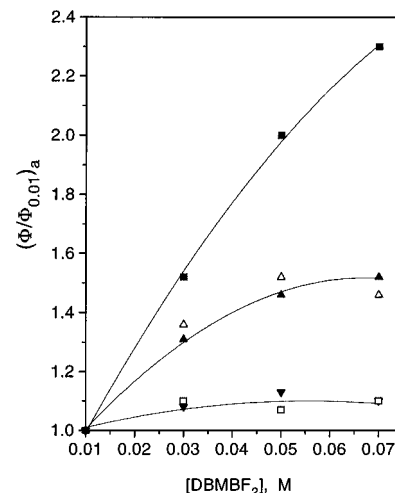


Figure 7. Plots of $(\Phi/\Phi_{0.01})_{\text{a}}$ vs [DBMBF₂]; CHD in dioxane (■) and benzene (□); 1,3-COD in dioxane (▲), CH₂Cl₂ (△) and benzene (▼).

much higher than K_{SV}^{m} (Table 3) obviously owing to the fact that ^{*}(DBMBF₂)₂ has a much longer lifetime^{3a} of 50 ns, and it is formed irreversibly since its dissociation rate constant is $< 2 \times 10^7 \text{ s}^{-1}$. This kinetic pattern implies that the excimer also reacts with dienes in nonaromatic solvents; this is substantiated by the increased $(\Phi/\Phi_{0.01})_{\text{a}}$ of **1** and **4** with increasing [DBMBF₂] as in Figure 7. The nearly flat plots of $(\Phi/\Phi_{0.01})_{\text{a}}$ in benzene demonstrate that the benzene exciplex is the sole reactive intermediate upon excitation, also showing that ^{*}(AA) is not formed in aromatic solvents. The mechanism will be discussed with monomer ^{*}DBMBF₂ as the model in nonaromatic solvents, and will be expanded later to association species.

In the exergonic region some substrates, such as quadricyclane, norbornadiene, and CHD, *etc.*, react with ^{*}DBMBF₂ to show extensive cation radical reactions, although a large number of substrates, while also undergoing electron transfer quenching under the conditions, does not give isolable reaction products. It is assumed that in the latter cases, reverse electron transfer ($k_{-\text{et}}$) in SSRIP is sufficiently fast to prevent separation (k_{sep}) and bulk cation radical reactions. Previous ESR studies^{4a} fail to reveal the presence of DBMBF₂^{•+} and/or olefin cation radicals, although the former was detected in the presence of the *tert*-butyldimethyl aminium radical as the counter cation. As we associate effective quenching distance, R_{eff} , in this region primarily with the electron jump to annihilate the excited state, R_{eff} must directly represent that of the collapse of the encounter complex to SSRIP. This interpretation is in agreement with the presence of radical ion reactions and the lack of new fluorescence as the consequence of long-range electron transfer with these substrates; the latter phenomenon arises from weak electronic coupling in SSRIP.

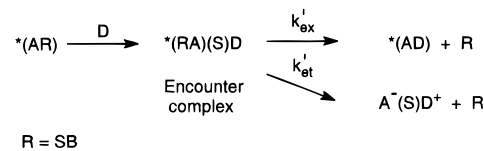
The calculated R_{eff} diminishes to about 3.0 Å on approaching the onset of the endergonic region, where the use of eq 2 is no longer valid;^{8a} the interaction is shifted now to exciplex formation. The close contact of reactants allows intermolecular bond formation and electronic coupling to occur, resulting in the cycloaddition to **1** and **4** and exciplex fluorescence; the latter is observed only with mesitylene or benzenes of higher E_{ox} where the charge transfer contribution^{4b} (CT %) is low and the locally excited state contribution (LE%) is high. As the center to center distance for linearly solvent separated reactants is about 7 Å, the calculated R_{eff} of 6–4 Å appears to be low, which could be understood in terms of a nonlinear arrangement of the solvent and reactants. In interaction with olefins, in spite of the observed scatter and lower calculated R_{eff} , the parameters could be modified to obtain better agreements; without such

refinements the point distribution indicates a parallel trend with SB substrates. We believe that *DBMBF_2 -olefin exciplexes, though nonemissive, are formed as the intermediate as supported by the observed symmetry controlled cycloadducts. There are only a few examples of using transient effects based on eq 2 in calculating R_{eff} to examine distance-dependent quenching.^{8d,e,g} In the present case, the extensive and systematic examples support the interpretation that R_{eff} indeed represents the separation of interacting *DBMBF_2 and substrates. With improved efficiency and accuracy of measuring R_{eff} , its correlation with $\Delta G_{\text{et}}^{\circ}$ (Figure 1B) should become more meaningful to describe the reaction dynamic than the correlation of k_{obs} which is a composite figure of various rate processes. However, k_{obs} is readily obtainable and Figure 1A can be easily constructed to show the control of free energy on electron transfer reactions;⁵ in the present case, it exhibits a transition region at which the fluorescence is quenched by competing processes of electron and energy transfer.

These conclusions require that in acetonitrile *DBMBF_2 be partitioned at the encounter complex as shown in Scheme 2 by k_{et} and k_{ex} processes. While the former long-range electron transfer is driven by the free energy of A/D pairs and medium polarity gradient, the latter follows the diffusion controlled dynamic by viscosity without being affected by these gradients.^{12a} The competition of the two processes depends on their activation energies and entropies that are obviously close enough to exhibit the observed dichotomy, which decides the variation of products under the conditions. For some systems involving singlet excited state quenchings in polar solvent, this mechanism has been proposed to explain faster decreases of fluorescence quantum yields, compared to those of measured lifetimes for exciplexes.^{5f,g,h,12e} Alternatively, it has been also suggested that such interactions lead totally to exciplexes with $\alpha = 1$, which are the key point of partition to various transformations.²⁰ Recently the Eastman Kodak group has published a series of excellent studies on the interaction of singlet excited dicyano- and tetracyanoanthracenes with SB.¹² They have applied elegant techniques to determine, among others, the efficiency of exciplex formation (from the relation of $\Phi_f/\tau = \alpha k_f$) by varying the donors and acceptors and solvent polarity.^{12a,e} It is pertinent to mention that, for these quenching reactions, $\alpha = 1$ in medium and less polar solvents for most of SB, but k_f decreases under the same conditions arising from increased CT% of exciplexes.^{12a} Our conclusion above agrees with their results that in acetonitrile $\alpha < 1$ and becomes lower with the decreasing redox energy ($E_{\text{redox}} = E_{\text{ox}} - E_{\text{red}}$) and higher polarity, *i.e.*, k_{et} is favored under these conditions. Similar conclusions also have been published.^{5h, 21}

The interaction of *DBMBF_2 and SB in the endergonic region is characterized by the formation of exciplexes that have been shown to be stabilized by electronic and resonance $|A^-D^+ \rangle \leftrightarrow |^*AD \rangle$ interactions. Their dipole moment measurements have yielded CT% ranging between 75 and 20% for those exciplexes derived from mesitylene to benzene.^{4b} With regard to the assumption that exciplexes are the precursors to cycloadducts **1** and **4**, a crucial question is the role played by CT and LE states in the cycloaddition process.²² We believe that CT does not serve as a driving force for the cycloaddition except to

Scheme 3



furnish ionic dipoles for regiospecific orientation. More quantitative studies are prevented by the intervention of electron transfer in the encounter stage as E_{redox} decreases in acetonitrile, effectively preventing exciplex formation. Since Φ_a of **1** and **4** increases in less polar solvents with concurrent LE% increases,^{4b} we conclude that the orbital symmetry controlled cycloaddition is driven by the LE component of the exciplex frontier orbital (*vide infra*). In acetonitrile, the *DBMBF_2 -1,3-COD exciplex, if formed, is estimated, from the oxidation potentials and CT% plot (ref 12a, Figure 5), to have the LE contribution $< 10\%$ (*i.e.*, CT% $> 90\%$); the quantum yield ($\Phi_a \approx 10^{-4}$) of **4** is indeed poor.

It follows that the redox energy, E_{redox} , exerts two effects in the present and allied singlet state photoreactions,¹² namely to provide driving force for long-range electron transfer in encounter pairs as well as to regulate the CT contribution in exciplexes. As the medium shifts from acetonitrile to less polar solvents, solvation energies diminish significantly. The extraordinary high fluorescence quantum yield of these *DBMBF_2 -SB exciplexes in cyclohexane^{4b} may arise from collapse of SSRIP if this is formed efficiently (Scheme 2). As cited above,^{12a,e} in medium to nonpolar solvents, a wide range of exciplexes are formed with high efficiency, $\alpha = 1$. The solvent effects summarised in Figures 3 and 5 demonstrate that in either pure or mixtures of nonaromatic nature (case I) and those of benzene-ether-type solvents (case II), Φ_a proportionally increases with the decreasing polarity; the increase must arise from the impediment of the k_{et} process, which results in the more exciplex formation. While there are scatters of points, the smooth variation shows that polarity effects override other factors such as specific solvent interactions and exciplex formations. In view of much higher K_{SV} of the corresponding exciplexes (in benzene, toluene or *p*-xylene)^{3a} by dienes in comparison to those in ether-type solvents, larger deviations for points involving aromatic solvents in the plots are expected. The lack of deviations demonstrates that a triplex involving SB is not likely involved in agreement with previous results.^{4b} Similar solvent effects have been observed in the photocycloaddition (on the product quantum yields)^{15,16} and in exciplex fluorescence rate constants and quantum yields.¹²⁻¹⁴

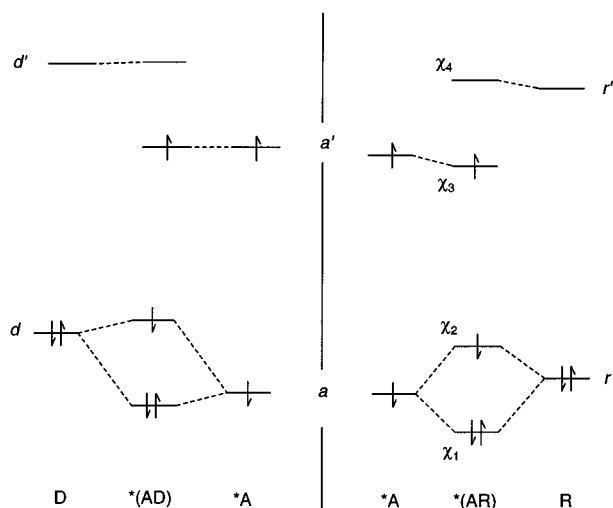
There exists a striking effect of *DBMBF_2 -SB exciplexes on the abrupt rises of dimer **2** quantum yields in acetonitrile; when *p*-xylene is added (case III), Φ_d is increased to the maximum by higher than an order of magnitudes (Figure 4) at 12 mol % ($[p\text{-xylene}] \approx ca. 1.12 \text{ M}$). A similar enhancement of Φ_d is also seen in the addition of toluene (1.28 M) and benzene (1.54 M), but not to the extent generated by *p*-xylene. The transient responsible for enhancement in acetonitrile must be *DBMBF_2 -SB exciplexes, but not likely the corresponding encounter pairs from the calculated $R_{\text{eff}} < 3.5 \text{ \AA}$ for all three cases. Also, from a published correlation^{12a} of $\Delta G_{\text{et}}^{\circ}$ vs $k_{\text{et}}/k_{\text{ex}}$, the three exciplexes are estimated to have $\alpha \approx 1$. Scheme 3 expresses the exciplexes $^*(AR)$ as the reactive intermediate, where R = SB.

(20) (a) Mataga, N.; Okada, T.; Yamamoto, N. *Chem. Phys. Lett.* **1967**, *1*, 119. (b) Okada, T.; Matsui, H.; Oohari, H.; Matsumoto, H.; Mataga, N. *J. Phys. Chem.* **1968**, *49*, 4771. (c) Mataga, N.; Murata, Y. *J. Am. Chem. Soc.* **1969**, *91*, 3144. (d) Mataga, N. *Pure Appl. Chem.*, **1984**, *56*, 1255.

(21) (a) Rau, H.; Frank, R.; Greiner, G. *J. Phys. Chem.* **1986**, *90*, 2476. (b) Stevens, B.; Biver, C. J., III; McKeithan, D. N. *Chem. Phys. Lett.* **1991**, *187*, 590. (c) Kikuchi, K.; Takahashi, Y.; Katagiri, T.; Niwa, T.; Hoshi, M.; Miyashi, T. *Chem. Phys. Lett.* **1991**, *180*, 403. (d) Kakitani, T.; Yoshimori, A.; Mataga, N. *J. Phys. Chem.* **1992**, *96*, 5385.

(22) (a) Lewis, F. D.; Hoyle, L. E. *J. Am. Chem. Soc.* **1977**, *99*, 2779. (b) Caldwell, R. A.; Creed, D. *J. Am. Chem. Soc.* **1979**, *101*, 6960. (c) Michl, J. *Photochem. Photobiol.* **1977**, *25*, 141. (d) Gerhartz, W.; Poshusta, R. O.; Michl, J. *J. Am. Chem. Soc.* **1976**, *98*, 6427.

Scheme 4



There is a parallel trend of the efficiency of $^*(AR)$ exciplex formations in acetonitrile (K_{SV} in Table 1) and of the calculated exciplex CT% (of *p*-xylene 76, toluene 51, and benzene 21%)^{4b} with the observed order of quantum yield enhancements. These results arise from the fact that DBMBF₂ has $E_{ox} = 2.45$ eV, which is below E_{ox} of toluene and *p*-xylene but above that of benzene (Table 1); electron transfer from former two to *DBMBF_2 should be easy but not from benzene. As the *DBMBF_2 -*p*-xylene exciplex possesses higher K_{SV} and CT%, it must form faster and undergo exciplex substitutions²³ with CHD (see Scheme 3) easier than the other two. The high medium polarity in acetonitrile is expected to provide favorable conditions for exciplex substitutions and also chain propagations. Such enhanced product yields in the presence of mediating donors have been reported in other systems, and interpreted as accelerated radical ion formation by an electron transfer relay process.^{23,24} Additionally, this may be ascribed to a superexchange interaction²⁵ in the encounter pair to facilitate long range electron transfer. Such interactions have been proposed to explain enhanced SSRIP formations^{12a,e} and, in the present case, may involve the encounter complex in Scheme 3 during exciplex substitutions^{23a,b} and possible triplex formation with CHD.^{23c} It is speculated that the approach of CHD in the encounter complex may have some regioselectivity to cause superexchange interactions favoring the SSRIP formation to account for enhanced Φ_d (Table 2A).

In this respect, the frontier MO scheme²⁶ can be used to qualitatively explain the quantum yield enhancement caused by the *p*-xylene exciplex in term of interplays between electron and orbital coupling at the HOMO–HOMO level; the LUMO–LUMO interaction is generally small. Owing to large HOMO–HOMO gap from CHD ($E_{ox} = 1.53$ eV, “*d*”) and *DBMBF_2 ($E_{ox} = 2.45$ eV, “*a*”) as shown in the left-hand side of Scheme 4, the interaction is purely electron transfer to give the contact radical ion pair (CRIP) if and when $^*(AD)$ is formed. Scheme 4 right-hand side gives the new MO of the DBMBF₂-*p*-xylene exciplex (shown as $^*(AR)$), χ_1 – χ_4 , that also shows that singly

occupied HOMO χ_2 is raised in energy to be closer to CHD HOMO “*d*”; this results in better electronic and orbital interactions between these two. Such improved interactions may be attributed to the driving forces to facilitate the substitutions shown in Scheme 3. Among three $^*(AR)$, the more polar *p*-xylene exciplex (*i.e.*, higher CT%) shows better electron interactions to promote the k'_{et} pathway; the benzene exciplex must have a χ_2 essentially similar to HOMO “*d*” of *DBMBF_2 and exerts very little effects.

The reaction of excimers, such as $^*(DBMBF_2)_2$, with substrates must be ubiquitous phenomena at high concentrations used in most preparative photochemistry. Since investigation of its role in the excited state reaction kinetics is not a trivial matter, quantum yield determinations in this kinetic study have been carried out with $[DBMBF_2] < 0.03$ M so that $^*(AA)$ concentrations are relatively small. Nevertheless, products resulting from excimer reactions can not be totally avoided especially at the onset of the photolysis. Both the kinetic as well as product patterns must be affected in complex ways by the various factors discussed above; one of them is the energy levels (redox and singlet excited states) of $^*(AA)$ that decide the free energy of electron transfer to the excimer from CHD, and that eventually determine the partition of its k'_{ex}/k'_{et} pathway ratio (*cf.* Scheme 3). In analogy to Scheme 4, the HOMO of $^*(AA)$ must be raised in the process of the excimer formation from the HOMO “*d*” of *DBMBF_2 to the new MO χ_2 , which is placed closer to the HOMO “*d*” of CHD; this must result in better electronic and orbital interactions²⁶ for the excimer and should perturb the k'_{ex}/k'_{et} ratio in analogous ways to that discussed above for exciplexes $^*(AR)$ (see Scheme 3). The increasing $(\Phi/\Phi_{0.01})_a$ vs $[DBMBF_2]$ plots indicate that these interactions between the excimer and CHD only promote the k'_{ex} pathway to give the exciplex and, in turn, cycloadduct **1**. As the excimer must possess close to zero CT%, the excimer substitution by electron transfer (k'_{et}) should be insignificant; the invariance of $(\Phi/\Phi_{0.01})_d$ even in polar solvent clearly support this argument. It is speculated that the HOMO–HOMO interaction of $^*(AA)$ and CHD may represent another type of superexchange enhancements in which the LE state interaction of the frontier orbitals provides the driving force.

The consistent conclusions drawn on the basis of Schemes 3 and 4 for both exciplex and excimer reactions indicate that the mechanistic proposals of this paper and the nature of reactive intermediates in previous papers^{3,4} can reasonably explain DBMBF₂ photoreactions.

Experimental Section

DBMBF₂, CHD, 1,3-COD, and SB were available from the previous work.^{1a} The absorption and fluorescence spectroscopy used the same apparatus, solvents and procedure as described before.^{4b}

The photoproducts **1**–**4** were identified before, and their GC analysis used authentic materials as the standard and calibration.^{3a} The solvents used in the quantum yield determinations were those supplied from Aldrich and distilled except ether which was anhydrous grade (Anachemia).

Acknowledgment. We wish to thank the Natural Sciences and Engineering Council of Canada, Ottawa, for generous support of this project. Z.-L.L. also gratefully acknowledges financial support from the National Science Foundation of China, Beijing.

Supporting Information Available: Table 2A giving the quantum yield of the DBMBF₂–CHD photoreaction in mixture solvents (4 pages). See any current masthead page for ordering and Internet access instructions.

(23) (a) Ohta, H.; Creed, D.; Wine, P. H.; Caldwell, R. A.; Melton, L. A. *J. Am. Chem. Soc.* **1976**, *98*, 2002. (b) Caldwell, R. A.; Creed, D.; Ohta, H. *J. Am. Chem. Soc.* **1975**, *97*, 3246. (c) Masaki, Y.; Uehara, Y.; Yanagida, S.; Pac, C. *J. Am. Chem. Soc.* **1990**, 1339.

(24) (a) Mattes, S. L.; Farid, S. *Acc. Chem. Res.* **1982**, *15*, 80. (b) Pac, C.; Nakasone, A.; Sakurai, H. *J. Am. Chem. Soc.* **1977**, *99*, 5806. (c) Majima, T.; Pac, C.; Nakasone, A.; Sakurai, H. *J. Am. Chem. Soc.* **1981**, *103*, 4499.

(25) (a) McConnell, H. M. *J. Chem. Phys.* **1961**, *35*, 508; (b) Miller, J. R.; Beitz, J. V. *J. Am. Chem. Soc.* **1981**, *74*, 6746.

(26) Michl, J.; Bonacic-Koutecky, V. *Electronic Aspects of Organic Photochemistry*; Wiley: New York, 1990; Chapter 5.